Distinct subdomains of the KCNQ1 S6 segment determine channel modulation by different KCNE subunits

Carlos G. Vanoye,[1] Richard C. Welch,[1] Melissa A. Daniels,[1] Lauren J. Manderfield,[2] Andrew R. Tapper,[2] Charles R. Sanders,[3] and Alfred L. George Jr.[1,2]

[1]Division of Genetic Medicine, Department of Medicine, [2]Department of Pharmacology, and [3]Department of Biochemistry, Center for Structural Biology, Vanderbilt University, Nashville, TN 37232

Modulation of voltage-gated potassium (K_V) channels by the KCNE family of single transmembrane proteins has physiological and pathophysiological importance. All five KCNE proteins (KCNE1–KCNE5) have been demonstrated to modulate heterologously expressed KCNQ1 (K_V7.1) with diverse effects, making this channel a valuable experimental platform for elucidating structure–function relationships and mechanistic differences among members of this intriguing group of accessory subunits. Here, we specifically investigated the determinants of KCNQ1 inhibition by KCNE4, the least well-studied KCNE protein. In CHO-K1 cells, KCNQ1, but not KCNQ4, is strongly inhibited by coexpression with KCNE4. By studying KCNQ1-KCNQ4 chimeras, we identified two adjacent residues (K326 and T327) within the extracellular end of the KCNQ1 S6 segment that determine inhibition of KCNQ1 by KCNE4. This dipeptide motif is distinct from neighboring S6 sequences that enable modulation by KCNE1 and KCNE3. Conversely, S6 mutations (S338C and F340C) that alter KCNE1 and KCNE3 effects on KCNQ1 do not abrogate KCNE4 inhibition. Further, KCNQ1-KCNQ4 chimeras that exhibited resistance to the inhibitory effects of KCNE4 still interact biochemically with this protein, implying that accessory subunit binding alone is not sufficient for channel modulation. These observations indicate that the diverse functional effects observed for KCNE proteins depend, in part, on structures intrinsic to the pore-forming subunit, and that distinct S6 subdomains determine KCNQ1 responses to KCNE1, KCNE3, and KCNE4.

The Journal of General Physiology

INTRODUCTION

Functional diversification of voltage-gated potassium (K_V) channels can be achieved in part through modulation by accessory subunits, including the KCNE proteins, a family of single transmembrane domain (TMD) proteins expressed in the heart, gut, kidney, brain, and other tissues (McCrossan and Abbott, 2004; Li et al., 2006). Many KCNE genes have been associated with various inherited or acquired cardiac arrhythmia syndromes (Abbott and Goldstein, 2002; Melman et al., 2002; Yang et al., 2004; Ma et al., 2007; Lundby et al., 2008; Ravn et al., 2008), indicating the physiological and pathophysiological importance of this gene family. Heterologous experiments have demonstrated that KCNE proteins are promiscuous and can alter the properties of many K_V channels (Abbott and Goldstein, 2002; McCrossan and Abbott, 2004; Li et al., 2006). In addition, certain K_V channels such as KCNQ1 (K_V7.1) are modulated by more than one type of KCNE protein with diverse effects (Bendahhou et al., 2005; Lundquist et al., 2005), and this specific channel has been adopted as an experimental model for elucidating the structural requirements and biophysical mechanisms underlying the effects of these accessory subunits. Determining how distinct patterns of channel modulation occur has important implications for understanding the role of KCNE proteins in health and disease.

KCNQ1 is a member of the K_V7 voltage-gated K^+ channel subfamily and, like other K_V channels, consists of a voltage-sensing domain formed by transmembrane segments S1–S4 and a pore domain composed of a pore loop and S5 and S6 helices. KCNQ1 gating, conductance, and pharmacology are radically altered by heterologous coexpression with KCNE proteins in vitro. A related K_V channel, KCNQ4 (K_V7.4), is also modulated by KCNE proteins but with very different outcomes. Coexpression of KCNE3 enhances KCNQ1 activity but inhibits KCNQ4 function (Schroeder et al., 2000; Strutz-Seebohm et al., 2006). Also, KCNE4 inhibits KCNQ1 but does not reduce KCNQ4 activity (Grunnet et al., 2002, 2005; Strutz-Seebohm et al., 2006). An analysis of divergent regions between KCNQ1 and KCNQ4 channels may help identify structures required for channel inhibition by KCNE4.

Here, we sought to identify primary structure differences between KCNQ1 and KCNQ4 that account for

Correspondence to Alfred L. George Jr.: al.george@vanderbilt.edu

A.R. Tapper's present address is Dept. of Psychiatry, University of Massachusetts, Worcester, MA 01655

Abbreviations used in this paper: HA, hemagglutinin; TMD, transmembrane domain.

The Rockefeller University Press $30.00
J. Gen. Physiol. Vol. 134 No. 3 207–217
www.jgp.org/cgi/doi/10.1085/jgp.200910234

their divergent responses to KCNE4. Our work demonstrated that a subdomain (V324-I328) within the extracellular end of S6 determines the KCNQ1 response to KCNE4, and this site is distinct from another S6 region that governs KCNQ1 modulation by KCNE1 and KCNE3. Further analysis revealed that a dipeptide motif (K326 and T327) accounts for the inhibitory response of KCNQ1 to KCNE4. Our studies also demonstrated that KCNE4 binding to KCNQ1 is not sufficient for the functional effects mediated through the S6 segment.

MATERIALS AND METHODS

Cell culture

Chinese hamster ovary cells (CHO-K1; CRL 9618; American Type Culture Collection) were grown in F-12 nutrient mixture medium (Invitrogen) supplemented with 10% FBS (ATLANTA Biologicals), penicillin (50 U × ml^{-1}), and streptomycin (50 µg × ml^{-1}) at 37°C in 5% CO_2. COS-M6 cells were grown at 37°C in 5% CO_2 in Dulbecco's modified Eagle's medium (Invitrogen) supplemented with 10% FBS, penicillin (50 units × ml^{-1}), streptomycin (50 µg × ml^{-1}), and 20 mM HEPES. Unless otherwise stated, all tissue culture media was obtained from Invitrogen.

Plasmids and cell transfection

Full-length human KCNQ1 (GenBank accession no. AF000571), KCNQ4 (AF105202), KCNE1 (L28168), and KCNE4 (AY065987) cDNAs were generated and engineered in the mammalian expression vectors pIRES2-EGFP (KCNQ1 and KCNQ4; BD) and a modified pIRES2 vector in which we substituted the fluorescent protein cDNA with that of DsRed-MST (provided by A. Nagy, University of Toronto, Toronto, Canada; pIRES2-DsRed-MST, KCNE1, and KCNE4) as described previously (Lundquist et al., 2005; Manderfield and George, 2008). Mutations were introduced into KCNQ1 and KCNQ4 using the QuikChange Site-Directed Mutagenesis system (Agilent Technologies). A triple hemagglutinin (HA) epitope (YPYDVPDYAGYPYDVPDYAGSYPYDVPDYA) was introduced into the KCNE4 cDNA immediately upstream of the stop codon as described previously (Manderfield and George, 2008). The epitope tag does not affect the functional effects of KCNE4 or its binding to KCNQ1 (Manderfield and George, 2008). A c-Myc–tagged KCNQ4 construct (provided by M. Shapiro, University of Texas Health Science Center at San Antonio, San Antonio, TX; Gamper et al., 2003) was used for detecting KCNQ4–KCNE4 interactions. All recombinant cDNAs were sequenced in their entirety to confirm the presence of the desired modifications and the absence of unwanted mutations.

Expression of KCNQ and KCNE constructs was achieved by transient plasmid transfection using FUGENE-6 (Roche) in which 2 µg of total cDNA was transfected with a KCNQ-KCNE mass ratio of 1:1. When the pore-forming subunit was expressed in the absence of KCNE subunits, the cells were cotransfected with the non-recombinant pIRES2-DsRed-MST vector alone. After transfection, cells were incubated for 48 h as described above before use in electrophysiological or biochemical experiments.

Biochemistry

All biochemical experiments including the preparation of cellular lysates, immunoprecipitation, and Western blotting were completed as described previously (Manderfield and George, 2008). In brief, 48 h after transfection, CHO-K1 cells were lysed with ice-cold NP-40 buffer (1% NP-40, 150 mM NaCl, and 50 mM Tris, pH 8.0) supplemented with a Complete mini-protease inhibitor (Roche). For immunoprecipitation, anti-KCNQ1 (Santa Cruz Biotechnology, Inc.) or anti-HA antibodies were chemically cross-linked to protein G Sepharose 4 Fast Flow (GE Healthcare) with dimethyl pimelimidate dihydrochloride (Sigma-Aldrich). Membranes were probed with anti-KCNQ1, anti-HA, and anti-GAPDH as described previously (Manderfield and George, 2008). Membranes probed with the c-Myc antibody (Covance) were incubated overnight with a 1:5,000 dilution of primary antibody and for 40 min with secondary antibody (1:5,000 dilution; horseradish peroxidase–conjugated goat anti–mouse; Santa Cruz Biotechnology, Inc.). Under the conditions used, we previously demonstrated that no protein–protein interactions occurred during the processing of cell lysates or that could be attributed to antibody cross-reactivity or nonspecific interactions with protein G Sepharose (Manderfield and George, 2008; Manderfield et al., 2009).

Coimmunoprecipitation of biotinylated membrane proteins

Cell surface biotinylation of COS-M6 cells was performed in 100-mm tissue culture dishes (three per condition), with cells grown to 70% confluence and transfected as described above. 48 h after transfection, the cells were washed twice with ice-cold Dulbecco's PBS (DPBS) supplemented with $CaCl_2$ and $MgCl_2$ (Invitrogen). After washing, cells were incubated in 3 ml DPBS plus 0.5 mg × ml^{-1} sulfo-NHS-SS-biotin, a cleavable and membrane-impermeant biotinylating reagent (Thermo Fisher Scientific) for 1 h on ice with shaking. The biotinylation solution was removed and the reaction was quenched by washing twice with DPBS with 50 mM Tris, pH 8.0, followed by two more washes with DPBS. The cells from one dish were lysed with ice-cold RIPA buffer (150 mM NaCl, 50 mM Tris-Base, pH 7.5, 1% IGEPAL, 0.5% sodium deoxycholate, and 0.1% SDS, supplemented with a Complete mini-protease inhibitor tablet [Roche]). After cell lysis, the supernatant was transferred to 1.5-ml microfuge tubes, vortexed for 20 s, rocked for 30 min at 4°C, and centrifuged at 14,000 *g* for 30 min. The supernatant fraction was collected and retained as the total lysate protein fraction. Samples were quantified using the Bradford reagent (Bio-Rad Laboratories), and equal amounts of proteins were used in the immunoprecipitation experiments. Aliquots of these supernatants were incubated with protein G Sepharose 4 Fast Flow to preclear nonspecific protein binding to the Sepharose beads. After this step, the supernatant was incubated with ImmunoPure Immobilized Streptavidin beads (Thermo Fisher Scientific) overnight at 4°C. The samples were centrifuged for 1 min at 14,000 *g*, and the supernatant fraction was collected and retained as the nonbiotinylated fraction.

The recovered streptavidin beads were washed with RIPA buffer three times for 5 min at 4°C. Then, the biotinylated proteins were eluted with RIPA buffer supplemented with 50 mM DTT for 2 h at room temperature to cleave the disulfide bond linking the covalently attached biotin moiety from streptavidin. The eluted sample was diluted to 1 ml with NP-40 buffer. Imunoprecipitation with anti-HA was performed as described previously (Manderfield and George, 2008). In control experiments, no protein was detected with anti-HA in nonbiotinylated membranes pulled down with streptavidin beads. All fractions were then subjected to Western blot analysis as described above, with the exception that all membranes were incubated overnight at 4°C with the appropriate primary antibody (1:200 anti-KCNQ1, 1:2,000 c-Myc 1:1,000 HA.11, or 1:2,000 GAPDH). All secondary antibodies were horseradish peroxidase conjugated, diluted to 1:5,000, and incubated at room temperature for 40 min. The c-Myc, HA.11, and GAPDH blots were probed with goat anti–mouse serum (Santa Cruz Biotechnology, Inc.), and KCNQ1[Q4S6]-F4 blots were probed with rabbit anti–goat serum (Santa Cruz Biotechnology, Inc.).

Electrophysiology

On the day of the experiment, transfected cells were dissociated by brief exposure to trypsin/EDTA, resuspended in supplemented

F-12 nutrient mixture medium, plated on glass coverslips, and allowed to recover for ~2 h at 37°C in 5% CO_2. Only yellow fluorescent cells (i.e., positive for both EGFP [successful KCNQ transfection] and DsRed-MST fluorescence [successful KCNE transfection]) were studied. Whole cell currents were recorded at room temperature (20–23°C) using Axopatch 200 and 200B amplifiers (MDS Analytical Technologies) in the whole cell configuration of the patch clamp technique (Hamill et al., 1981). Pulse generation was done with Clampex 8.0 (MDS Analytical Technologies), and whole cell currents were filtered at 1 kHz and acquired at 5 kHz. The access resistance and apparent membrane capacitance were estimated using an established method (Lindau and Neher, 1988). Whole cell currents were not leak subtracted. Whole cell currents were measured from −80 to +60 mV (in 10-mV steps) 1,990 ms after the start of the voltage pulse from a holding potential of −80 mV. The external solution contained (in mM): 132 NaCl, 4.8 KCl, 1.2 $MgCl_2$, 1 $CaCl_2$, 5 glucose, and 10 HEPES, pH 7.4. And the internal solution contained (in mM): 110 K^+ aspartate, 1 $CaCl_2$, 10 HEPES, 11 EGTA, 1 $MgCl_2$, and 5 K_2ATP, pH 7.3. Pipette solution was diluted 5–10% to prevent activation of swelling-activated currents. Patch pipettes were pulled from thick-wall borosilicate glass (World Precision Instruments, Inc.) with a multistage P-97 Flaming-Brown micropipette puller (Sutter Instrument Co.) and heat polished with a Micro Forge MF 830 (Narashige). After heat polishing, the resistance of the patch pipettes was 3–5 MΩ in the standard extracellular solution. The access resistance varied from 3 to 9 MΩ, and experiments were excluded from analysis if the voltage errors originating from the series resistance were >5 mV. As a reference electrode, a 2% agar bridge with composition similar to the control bath solution was used. Junction potentials were zeroed with the filled pipette in the bath solution. Unless otherwise stated, all chemicals were obtained from Sigma-Aldrich.

Data analysis

Data were collected for each experimental condition from at least three transient transfections and analyzed and plotted using a combination of Clampfit (MDS Analytical Technologies) and SigmaPlot 2000 (Systat Software, Inc.). Statistical analyses were performed using SigmaStat 2.03 (Systat Software, Inc.), and p-values are listed in the figure legends. Statistical significance among two groups was determined using the unpaired Student's *t* test, and one-way ANOVA followed by a Tukey post-test was performed when comparing more than two groups (Fig. 6). Whole cell currents are normalized for membrane capacitance, and results are expressed as mean ± SEM. The number of cells used for each experimental condition is given in the figure legends.

RESULTS

KCNQ1 S6 segment determines inhibition by KCNE4

Previous heterologous expression experiments in *Xenopus* oocytes demonstrated that KCNE4 inhibits KCNQ1 (Grunnet et al., 2002, 2005), but not KCNQ4 (Grunnet et al., 2002; Strutz-Seebohm et al., 2006). Similarly in CHO-K1 cells, transient coexpression of KCNE4 also inhibited KCNQ1-induced currents but did not reduce whole cell currents in KCNQ4-expressing cells (Fig. 1). The distinct responses of KCNQ1 and KCNQ4 motivated our present study using KCNQ1/KCNQ4 chimeras to determine the structural requirements for KCNE4 inhibition of channel activity. Prior studies have suggested that the KCNQ1 S6 segment (denoted as KCNQ1-S6)

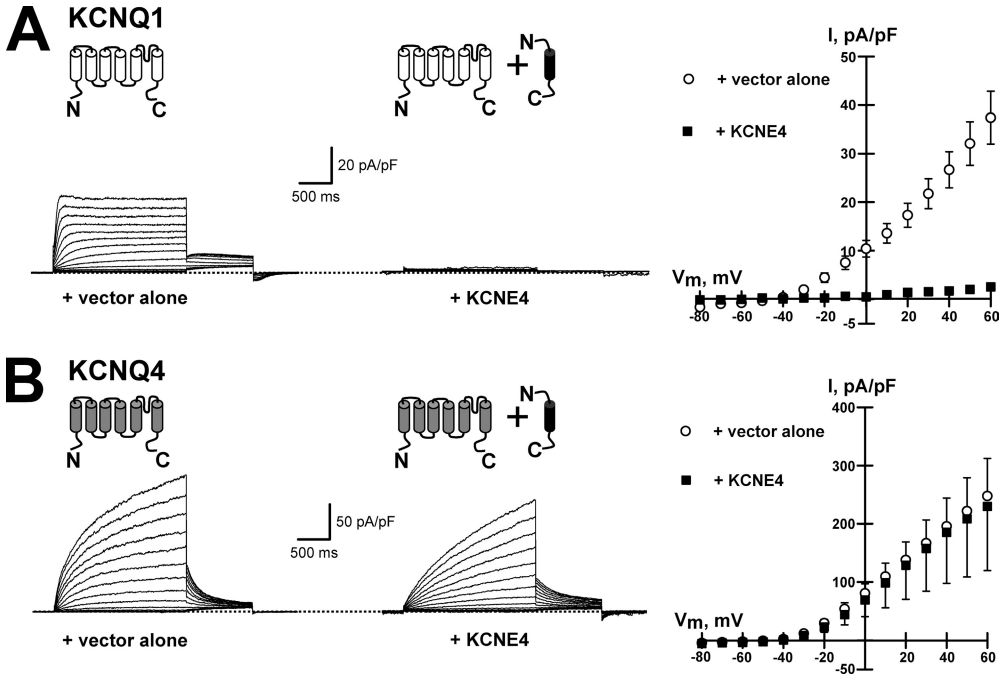

Figure 1. KCNE4 inhibits KCNQ1, but not KCNQ4, channels. (A) Representative whole cell currents recorded from cells cotransfected with KCNQ1 plus either empty plasmid vector (left) or KCNE4 (middle). The right panel shows the average I-V relationship measured after 2-s pulses from cells expressing KCNQ1 alone (○) and KCNQ1 plus KCNE4 (■). (B) Whole cell currents recorded from cells cotransfected with KCNQ4 plus either empty plasmid vector (left) or KCNE4 (middle). The right panel illustrates the average I-V relationship from cells expressing KCNQ4 alone (○) and KCNQ4 plus KCNE4 (■). Recordings were made from 11–14 cells for each condition. p-values for KCNQ1 alone and KCNQ1 plus KCNE4 comparisons are <0.005 from −30 to +60 mV. In this and subsequent figures, the dotted lines in the representative traces indicate zero current.

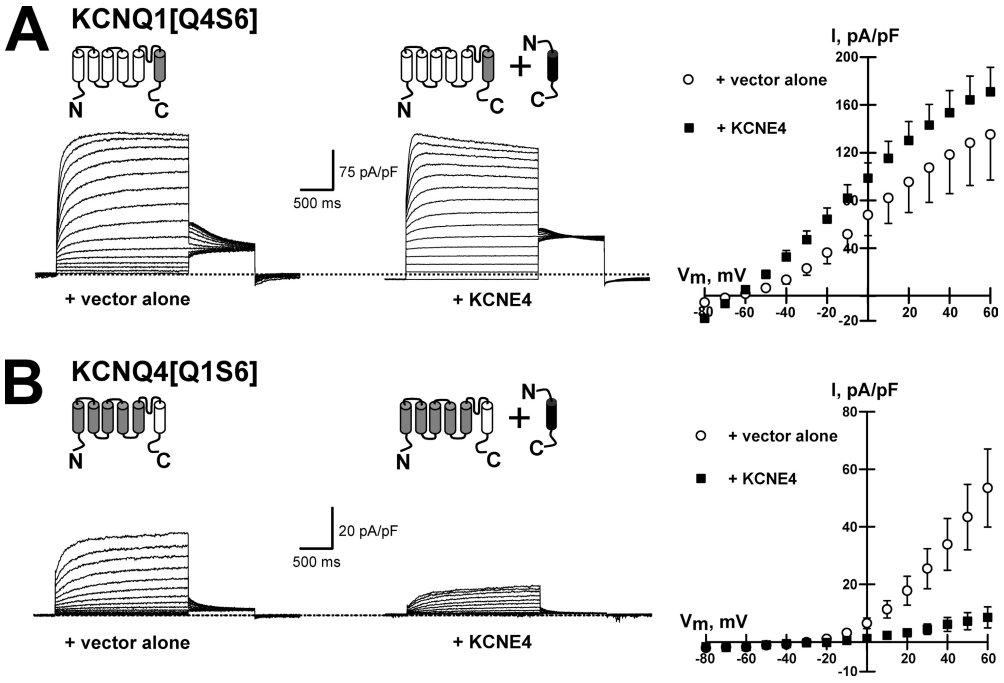

Figure 2. The KCNQ1-S6 segment confers KCNE4 sensitivity. (A) Representative whole cell currents and I-V relationships recorded from cells coexpressing KCNQ1[Q4S6] with either KCNE4 (■) or empty plasmid vector (○). (B) Whole cell currents and I-V relationships recorded from cells coexpressing KCNQ4[Q1S6] with either KCNE4 (■) or empty plasmid vector (○). The diagrams above the current traces illustrate the chimera composition: open cylinders represent KCNQ1 transmembrane segments, and gray cylinders represent KCNQ4 transmembrane segments. Recordings were made from six to nine cells for each condition. p-values for KCNQ1[Q4S6] alone and KCNQ1[Q4S6] plus KCNE4 comparisons are <0.05 from −10 to −80 mV, and ≤0.03 from 0 to +60 mV for KCNQ4[Q1S6] alone and KCNQ4[Q1S6] plus KCNE4 comparisons.

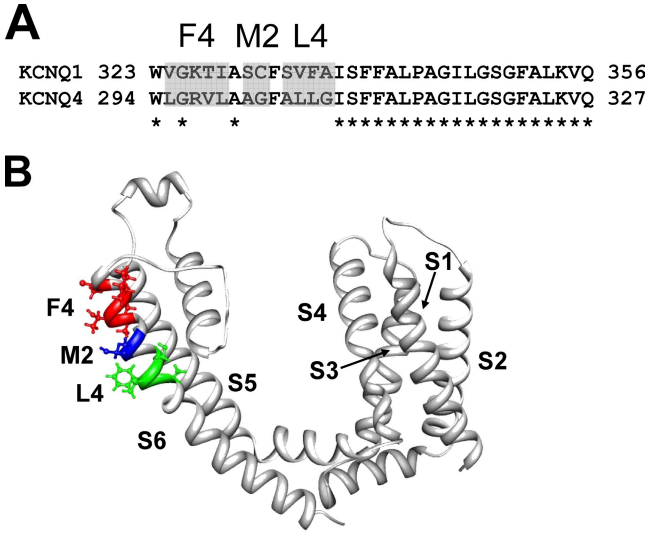

Figure 3. Divergent residues between KCNQ1 and KCNQ4 S6 segments. (A) Amino acid alignment of KCNQ1 and KCNQ4 S6 segments. The divergent residues are arbitrarily divided into three subregions: F4 (V324, K326, T327, and I328), M2 (S330 and C331), and L4 (S333, V334, F335, and A336). Asterisks indicate amino acid identities between the S6 segments. (B) Spatial location of the KCNQ1-S6/KCNQ4-S6 divergent residues in KCNQ1-S6 is illustrated using a monomeric KCNQ1 homology model rendered using CHIMERA software and based upon a previously published model (Smith et al., 2007).

and the TMD of KCNE1 interact functionally or lie in close proximity within the assembled channel complex (Tai and Goldstein, 1998; Tapper and George, 2001; Melman et al., 2004; Panaghie et al., 2006; Kang et al., 2008; Chung et al., 2009). Based upon these observations, we hypothesized that specific primary structure differences between KCNQ1 and KCNQ4 S6 segments account for the distinct effects of KCNE4 on these channels.

To test whether the S6 segment is critical for KCNE4 inhibition of channel function, a KCNQ1 chimera containing the S6 sequence of KCNQ4 (denoted KCNQ1[Q4S6]) was constructed and transiently coexpressed with KCNE4 in CHO-K1 cells. The results presented in Fig. 2 A indicate that, in contrast to wild-type KCNQ1 channels, KCNQ1[Q4S6] channels are not inhibited by KCNE4. The role of KCNQ1-S6 in mediating the response to KCNE4 is supported by the converse chimera in which the S6 segment of KCNQ4 was replaced with that of KCNQ1 (KCNQ4[Q1S6]). Unlike wild-type KCNQ4, KCNQ4[Q1S6] channels are inhibited by KCNE4 coexpression (Fig. 2 B). These results supported our hypothesis that critical determinants of KCNQ1 inhibition by KCNE4 reside within the S6 segment and can be transferred to KCNQ4 to confer an inhibitory response.

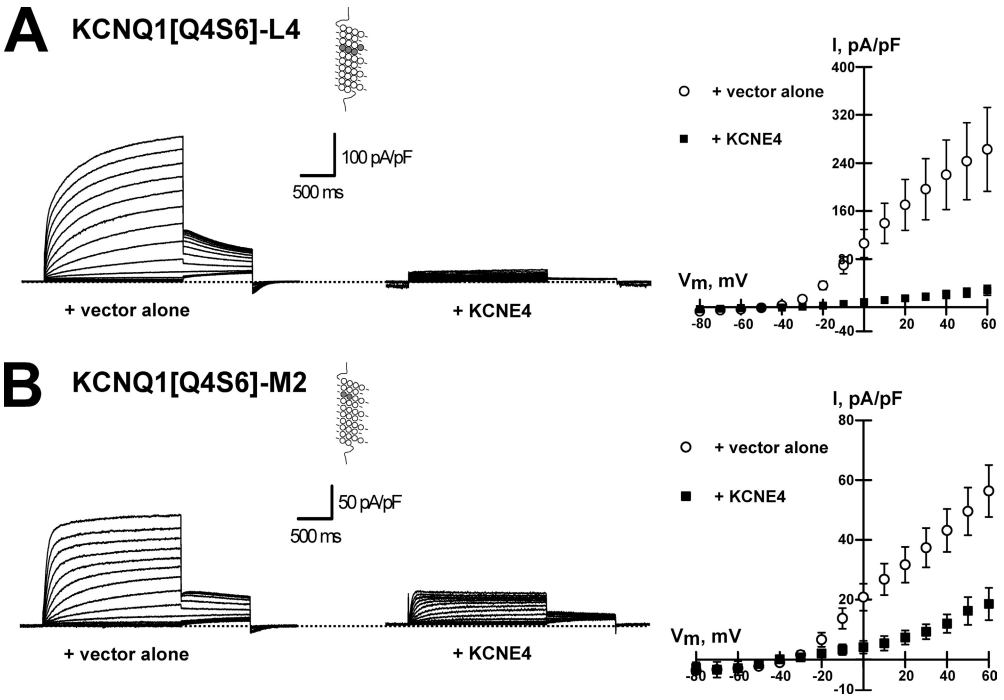

Figure 4. Substitution of lower and middle divergent regions of KCNQ1-S6 does not prevent KCNE4 inhibition. Representative whole cell current traces and I-V relationships recorded from cells expressing KCNQ1[Q4S6]-L4 (A) or KCNQ1[Q4S6]-M2 (B) chimeras cotransfected with either KCNE4 (■) or empty plasmid vector (○). The diagrams illustrate the location of the substituted residues from KCNQ4-S6 (shaded circles) in the KCNQ1-S6 background (○). Recordings were made from six to seven cells for each condition. The p-values for KCNQ1[Q4S6]-L4 alone and KCNQ1[Q4S6]-L4 plus KCNE4 comparisons are ≤0.006 from −30 to +60 mV, and ≤0.007 from 0 to +60 mV for KCNQ1[Q4S6]-M2 alone and KCNQ1[Q4S6]-M2 plus KCNE4 comparisons.

Distinct regions of KCNQ1-S6 determine effects of KCNE1, KCNE3, and KCNE4

There are 10 residues that differ between the S6 segments of KCNQ1 and KCNQ4 (Fig. 3 A). In KCNQ1, the divergent residues are located between valine-324 (V324) and alanine-336 (A336), and their location in the KCNQ1 channel is depicted in Fig. 3 B using a monomeric KCNQ1 homology model (Smith et al., 2007). The divergent residues were arbitrarily divided into three subregions labeled F4 (first four divergent residues), M2 (middle two divergent residues), and L4 (last four divergent residues). To determine which divergent residues between KCNQ1 and KCNQ4 S6 segments are critical for inhibition by KCNE4, KCNQ1 chimeras incorporating each of the three divergent subregions from KCNQ4-S6 were generated and coexpressed with KCNE4.

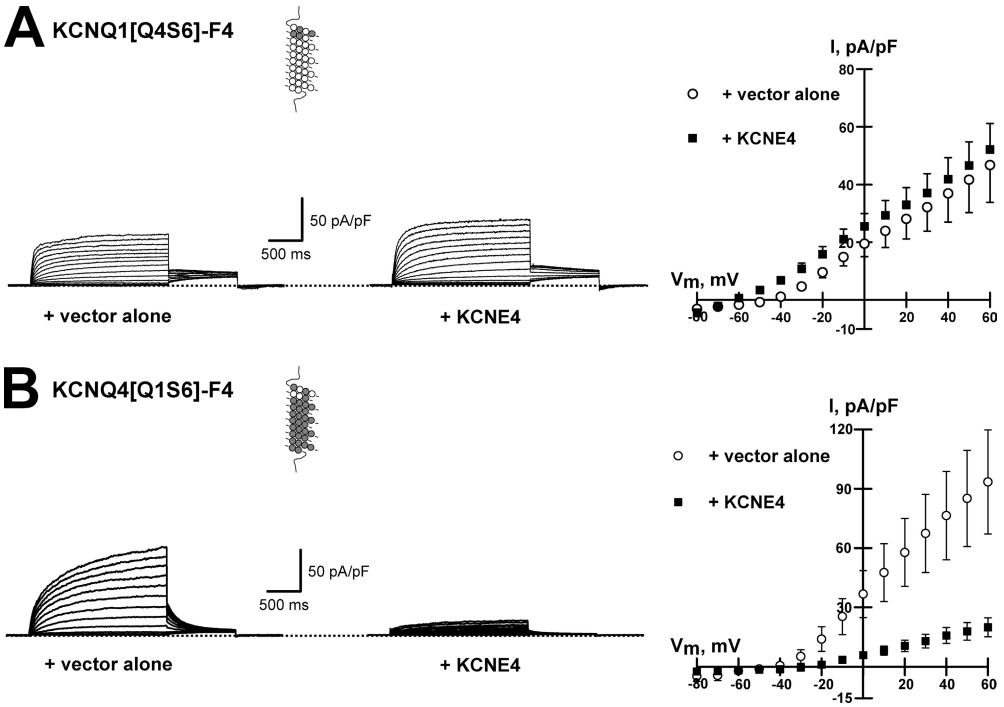

Figure 5. The extracellular end of KCNQ1-S6 confers KCNE4 inhibition. (A) Representative whole cell current traces and I-V relationships recorded from cells expressing KCNQ1[Q4S6]-F4 channels plus either KCNE4 (■) or empty plasmid vector (○). (B) Whole cell current traces and I-V relationships recorded from cells expressing KCNQ4[Q1S6]-F4 plus either KCNE4 (■) or empty plasmid vector (○). The diagrams illustrate the location of the substituted residues, with KCNQ1-S6 residues shown as open circles and KCNQ4-S6 residues shown as shaded circles. Recordings were made from 10–12 cells for each condition. The p-values for KCNQ4[Q1S6]-F4 alone and KCNQ4[Q1S6]-F4 plus KCNE4 comparisons are ≤0.02 from +10 to +60 mV, and ≤0.03 from −10 to 0 mV.

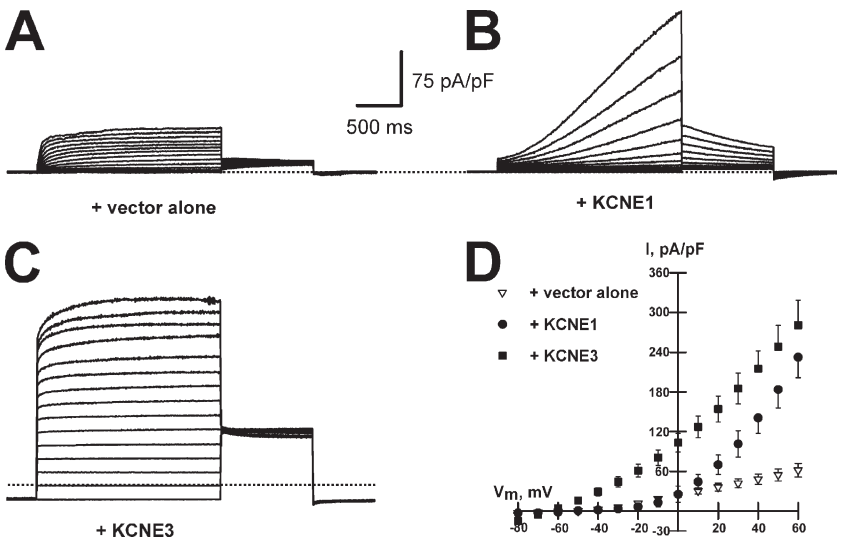

Figure 6. KCNQ1[Q4S6]-F4 channels exhibit intact KCNE1 and KCNE3 modulation. Representative whole cell currents recorded from cells coexpressing KCNQ1[Q4S6]-F4 with empty vector (A), KCNE1 (B), or KCNE3 (C). (D) Average I-V relationships from cells coexpressing KCNQ1[Q4S6]-F4 with empty vector (▽; n = 15), KCNE1 (●; n = 7), or KCNE3 (■; n = 6). The p-values for KCNQ1[Q4S6]-F4 alone and KCNQ1[Q4S6]-F4 plus KCNE1 or KCNQ1[Q4S6]-F4 plus KCNE3 comparisons are ≤0.001 from +10 to +60 mV (one-way ANOVA).

Fig. 4 illustrates representative whole cell currents recorded from CHO-K1 cells transiently expressing KCNQ1[Q4S6]-L4 (substitutions of S333-A336) and KCNQ1[Q4S6]-M2 (substitutions of S330-C331) in the absence or presence of KCNE4. Substitution of the lower (KCNQ1[Q4S6]-L4) and middle (KCNQ1[Q4S6]-M2) divergent subregions of KCNQ1-S6 with the corresponding amino acids from KCNQ4 did not prevent KCNE4 from inhibiting whole cell currents (Fig. 4, A and B). In contrast, whole cell currents recorded from cells expressing KCNQ1[Q4S6]-F4 (substitutions of V324-I328) were not suppressed by KCNE4 (Fig. 5 A). These findings indicated that an important determinant of KCNQ1 inhibition by KCNE4 is located within the extracellular end of the S6 segment between amino acids V324 and I328. This conclusion is strengthened by the results obtained with the converse KCNQ4 chimera (KCNQ4[Q1S6]-F4) in which only the F4 subregion residues were replaced with those of KCNQ1. In contrast with its effect on wild-type KCNQ4, coexpression of KCNE4 significantly reduced KCNQ4[Q1S6]-F4 current density (Fig. 5 B), indicating that we can transfer inhibitory responsiveness to KCNQ4.

Although substitution of the four most extracellular divergent residues in the S6 segment of KCNQ1 (V324-I328) prevented channel inhibition by KCNE4, these substitutions did not generate a completely KCNE-insensitive channel. Coexpression of KCNQ1[Q4S6]-F4 with KCNE1 generated slowly activating currents similar to those observed when KCNE1 is coexpressed with

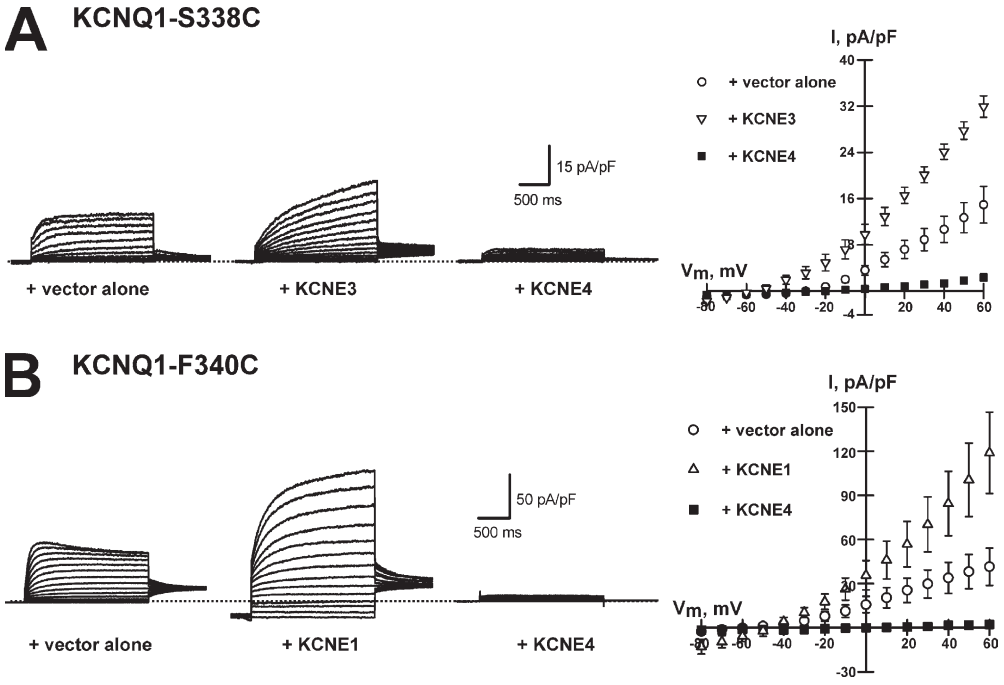

Figure 7. KCNQ1-S338C and KCNQ1-F340C mutants are inhibited by KCNE4. (A) Representative whole cell currents and I-V relationships recorded from cells coexpressing KCNQ1-S338C with either empty plasmid vector (○; n = 11), KCNE3 (▽; n = 6), or KCNE4 (■; n = 7). The p-values for the difference between KCNQ1-S338C alone or with KCNE4 coexpression are ≤0.01 from 0 to +60 mV. (B) Representative whole cell currents and I-V relationships recorded from cells coexpressing KCNQ1-F340C with either empty vector (○; n = 11), KCNE1 (△; n = 6), or KCNE4 (■; n = 9). The p-values for the difference between KCNQ1-F340C alone or with KCNE4 coexpression are ≤0.02 from 0 to +60 mV.

wild-type KCNQ1 (Fig. 6 B) (Barhanin et al., 1996; Sanguinetti et al., 1996). Similarly, coexpression of this chimera with KCNE3 generated rapidly activating currents with a linear I-V relationship also resembling the effects on wild-type KCNQ1 (Fig. 6 C) (Schroeder et al., 2000; Melman et al., 2001). These results imply that the KCNQ1 S6 segment contains residues critical for the channel response to KCNE4, but that these residues are distinct from those reported to enable modulation by KCNE1 and KCNE3 (Melman et al., 2004; Panaghie et al., 2006). We corroborated this observation by testing KCNE4 effects on two specific KCNQ1 point mutants, KCNQ1-S338C and KCNQ1-F340C, previously shown to alter KCNQ1 modulation by KCNE1 and KCNE3, respectively (Melman et al., 2004). Fig. 7 illustrates that although these mutant channels exhibit altered sensitivity to KCNE3 (KCNQ1-S338C) and KCNE1 (KCNQ1-F340C), both were inhibited by KCNE4 coexpression. These data provide further support for the hypothesis that distinct S6 subdomains influence KCNQ1 responses to KCNE1, KCNE3, and KCNE4.

Subunit binding is not sufficient for KCNQ1 inhibition by KCNE4

Previous work from our laboratory demonstrated that KCNE4 biochemically interacts with KCNQ1 (Manderfield and George, 2008). Therefore, a plausible explanation for the failure of KCNE4 to modulate KCNQ1[Q4S6]-F4 is impaired KCNE4 binding to the channel. To test this idea, whole cell lysates were obtained from CHO-K1 cells transiently transfected with HA epitope–tagged KCNE4 and either wild-type KCNQ1 or KCNQ1[Q4S6]-F4. The lysates were immunoprecipitated with anti-KCNQ1 and then subjected to SDS-PAGE, followed by Western blot analysis to detect KCNQ1 and KCNE4 proteins. Fig. 8 A illustrates that KCNE4 can be coimmunoprecipitated with both wild-type KCNQ1 and KCNQ1[Q4S6]-F4. These results demonstrate that the substitution of the four residues (V324-I328L) in KCNQ1[Q4S6]-F4 makes the channel resistant to block by KCNE4 but does not prevent binding of this accessory subunit to the channel. These results indicate that the physical interactions between KCNE4 and KCNQ1 that enable coimmunoprecipitation are not sufficient to mediate the inhibitory effects of KCNE4.

We also examined biochemical interactions between KCNE4 and KCNQ4. Whole cell lysates were obtained from CHO-K1 cells transiently transfected with HA epitope–tagged KCNE4 and c-Myc epitope–tagged KCNQ4 (Gamper et al., 2003). The lysates were immunoprecipitated with anti-HA and then subjected to SDS-PAGE, followed by Western blot analysis to detect KCNQ4 and KCNE4 proteins. Fig. 8 B illustrates that KCNE4 can be coimmunoprecipitated with wild-type KCNQ4 despite the absence of functional modulation of current carried by these channels (Fig. 1 B).

The biochemical association of KCNE4 with either KCNQ1[Q4S6]-F4 or KCNQ4 in the absence of a functional effect on either channel could indicate that the heteromeric complexes do not reach the plasma membrane, and that only homomeric KCNQ1[Q4S6]-F4 or KCNQ4 channels are present at the cell surface to conduct current. To test whether KCNQ1[Q4S6]-F4–KCNE4 or KCNQ4–KCNE4 protein complexes are present at the plasma membrane, we performed coimmunoprecipitation experiments on biotinylated membrane proteins. These experiments were conducted in COS-M6 cells because of the higher protein expression needed for sequential protein isolation (i.e., recovery of

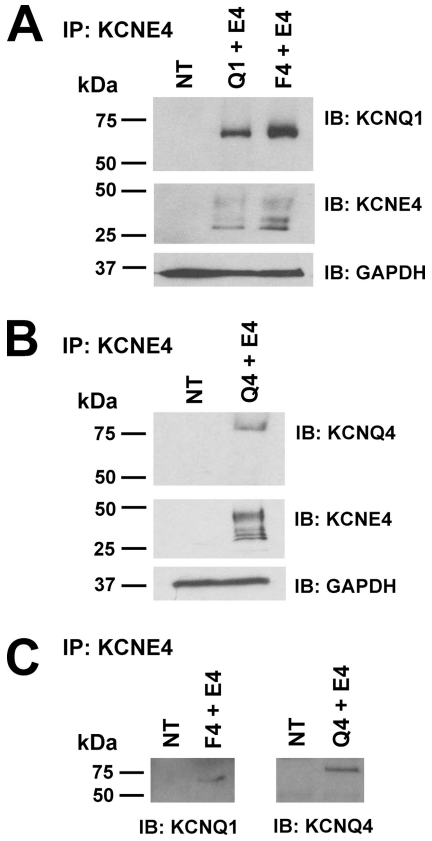

Figure 8. Coimmunoprecipitation of KCNE4, KCNQ1(Q4S6)-F4, and KCNQ4. (A) The top and middle panels illustrate whole cell lysate proteins immunoprecipitated with an anti-HA antibody (to recover HA-tagged KCNE4) and then probed with anti-KCNQ1 antibody (top) or with anti-HA tag antibody (middle). NT, nontransfected cells; Q1 + E4, cells transfected with KCNQ1 and KCNE4-HA; F4 + E4, cells transfected with KCNQ1[Q4S6]-F4 and KCNE4-HA. (B) The top and middle panels illustrate whole cell lysate proteins immunoprecipitated with anti-HA and then probed with c-Myc antibody to detect KCNQ4 (top) or with anti-HA to detect KCNE4 (middle). NT, nontransfected cells; Q4 + E4, cells transfected with c-Myc-KCNQ4 and KCNE4-HA. The bottom panels in A and B are GAPDH immunoblots of the initial whole cell lysates demonstrating total protein expression. (C) Biotinylated membrane proteins immunoprecipitated with anti-HA and then probed with KCNQ1 antibody (left) to detect KCNQ1[Q4S6]-F4 or c-Myc antibody to detect KCNQ4 (right).

biotinylated proteins with streptavidin followed by immunoprecipitation). Fig. 8 C illustrates that KCNQ4 and KCNQ1[Q4S6]-F4 can be coimmunoprecipitated with KCNE4 from membrane protein fractions. Biotinylated protein fractions did not contain intracellular proteins based on the observation that GAPDH was only detected in the total lysate and nonbiotinylated lanes, but not in the biotinylated fraction (not depicted). These observations indicate that both KCNQ1[Q4S6]-F4 and KCNQ4 channels can bind KCNE4 and reach the plasma membrane, implying that biochemical interactions between KCNE4 and these channels are not sufficient for the inhibitory effects of this KCNE subunit. Moreover, our coimmunoprecipitation results after protein elution in the presence of 50 mM DTT (see Materials and methods) suggest that disulfide bonds are not required to maintain the KCNQ1[Q4S6]-F4–KCNE4 or KCNQ4–KCNE4 protein complexes.

KCNQ1-S6 dipeptide enables inhibition by KCNE4

To further delimit the region in KCNQ1-S6 critical for inhibition by KCNE4, we individually substituted the four residues within the F4 region with the corresponding amino acids from KCNQ4. Fig. 9 (A and B) illustrates representative whole cell currents recorded from CHO-K1 cells transiently expressing the single mutant KCNQ1 channels KCNQ1-V324L, KCNQ1-K326R, KCNQ1-T327V, or KCNQ1-I328L in the absence or presence of KCNE4. All mutant channels generated whole cell currents similar to wild-type KCNQ1. Functional analysis of the single mutant KCNQ1 channels coexpressed with KCNE4 indicated that the two central residues within the F4 subdomain are critical for KCNE4 inhibition of channel activity. Substitution of either lysine 326 by arginine or threonine 327 by valine was sufficient to disrupt KCNE4 inhibition of KCNQ1. As predicted from the results with KCNQ1[Q4S6]-F4 (Fig. 6 B), coexpression of each single KCNQ1 mutant with KCNE1 generated I_{Ks}-like currents (not depicted). Collectively, these results indicate that the sensitivity of KCNQ1 to KCNE4, but not to KCNE1, is determined by a dipeptide (lysine-threonine) motif near the extracellular end of KCNQ1-S6.

The relevance of residues K326 and T327 in KCNE4 sensitivity is underscored by the fact that only KCNQ1 has these specific amino acids and is the only K_V7 channel inhibited by KCNE4 (Grunnet et al., 2002). In place of lysine, the other four KCNQ channels have arginine at this position. And instead of threonine, KCNQ4 has valine, whereas KCNQ2-3 and KCNQ5 possess leucine

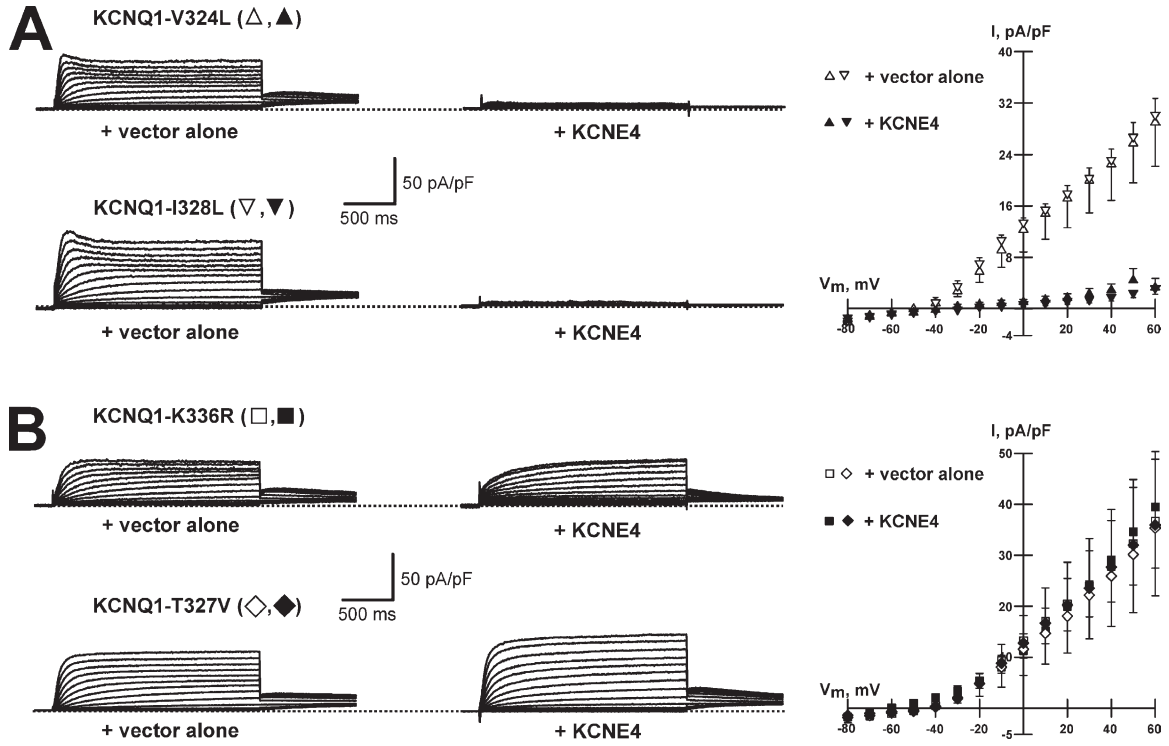

Figure 9. Dipeptide motif unique to KCNQ1-S6 enables KCNE4 inhibition. (A) Representative whole cell currents recorded from cells expressing the KCNE4-sensitive mutants KCNQ1-V324L (△) and KCNQ1-I328L (▽) alone or with KCNE4 and corresponding average I-V plots determined in the presence (▲; $n = 6$; ▼; $n = 7$) or absence (△; $n = 6$; ▽; $n = 7$) of KCNE4. The p-values are ≤0.013 from −20 to +60 mV for KCNQ1-V324L alone compared with KCNQ1-V324L plus KCNE4, and ≤0.001 from −30 to +60 mV for KCNQ1-I328L alone compared with KCNQ1-I328L plus KCNE4. (B) Representative whole cell currents recorded from cells expressing the KCNE4-resistant mutants KCNQ1-K326R (□) and KCNQ1-T327V (◇) alone or with KCNE4, and corresponding average I-V plots determined in the presence (■; $n = 9$; ◆; $n = 7$) or absence (□; $n = 12$; ◇; $n = 5$) of KCNE4.

(Fig. 10 A). A helical wheel depiction of KCNQ1-S6 (Fig. 10 B) illustrates that the two residues most critical for KCNE4 inhibition (K326 and T327, indicated by solid arrows) are present along a surface-exposed face of the helix, whereas the residues (V324 and I328L) that do not affect KCNE4 sensitivity reside at the opposite side of the helix. The helical depiction of the KCNQ1 S6 segment places K326 and T327 on similar faces as F340 and S338 (Fig. 10 B, filled circles), residues critical for KCNE1 and KCNE3 modulation of KCNQ1 activity (Melman et al., 2004; Panaghie et al., 2006). Although the four residues have similar orientation, K326 and T327 are separated three to four α-helical turns away from F340 and S338.

DISCUSSION

Many important questions remain unanswered regarding the structural determinants and functional mechanisms by which KCNE proteins exert diverse effects on K_V channels (Abbott et al., 2001; McCrossan and Abbott, 2004; Li et al., 2006). Prior work suggests that the TMDs of KCNE1, KCNE2, and KCNE3 interact with the S1, S4, and S6 segments and the S4–S5 linker of KCNQ1 to mediate functional effects (Tai and Goldstein, 1998; Tapper and George, 2001; Melman et al., 2004; Panaghie et al., 2006; Kang et al., 2008; Restier et al., 2008; Shamgar et al., 2008; Xu et al., 2008; Chung et al., 2009). In contrast, no information exists regarding structures required for KCNQ1 inhibition by KCNE4.

In this study, we determined that divergent residues in the S6 segments of KCNQ1 and KCNQ4 account for differences in their responses to KCNE4. These experiments exploited the observations that KCNQ1, but not KCNQ4, is strongly inhibited by this accessory subunit (Grunnet et al., 2002, 2005; Strutz-Seebohm et al., 2006). Our findings indicated that a dipeptide sequence at the extracellular (outer) end of S6 correlates with the distinct KCNE4 effects on KCNQ1 and KCNQ4. Although mutations in the outer S6 segment were sufficient to prevent KCNQ1 inhibition by KCNE4, these structural changes did not impair biochemical interactions between the two subunits, thus illustrating that accessory subunit binding alone is not sufficient for the inhibitory effects of KCNE4.

We further demonstrated that the outer region of KCNQ1-S6 accounts for the dramatic response to KCNE4 but does not alter KCNQ1 modulation by KCNE1 or KCNE3. Previous studies have demonstrated that residues located toward the cytoplasmic end of KCNQ1-S6 (S338-F340) are critical for channel modulation by KCNE1 and KCNE3 (Melman et al., 2004; Panaghie et al., 2006). Our results imply that KCNQ1-S6 contains specialized subdomains that separately enable activation by KCNE1 and KCNE3 (residues 338–340) or inhibition by KCNE4 (residues 326–327).

Mechanistic implications

At least two plausible mechanisms involving either gating or permeation can be conceived to explain the

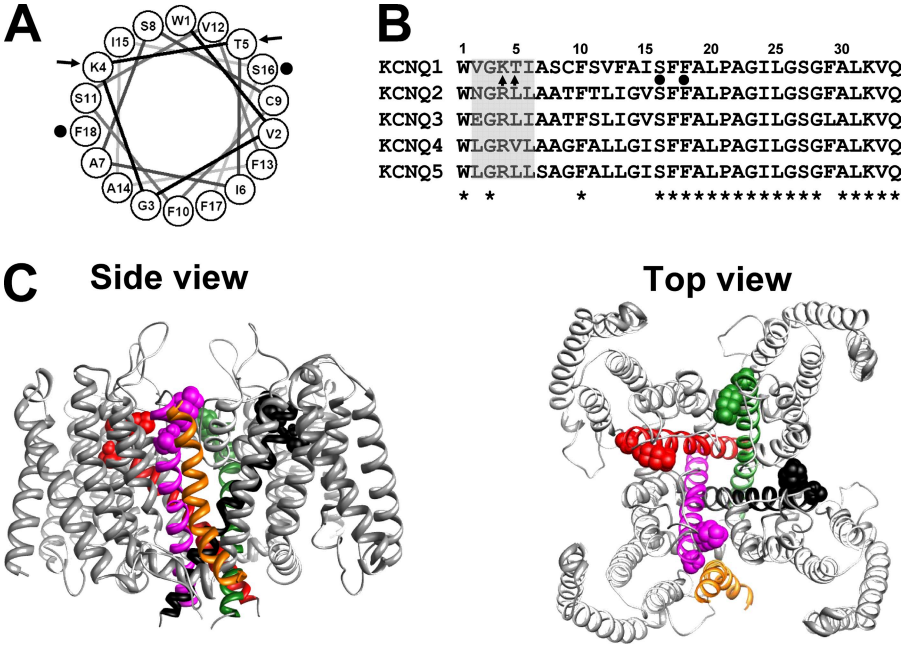

Figure 10. Location of K326 and T327 in a KCNQ1-KCNE1 closed-state model. (A) Amino acid alignment of S6 segments from all KCNQ channels with the divergent F4 subregion denoted with a shaded box. Asterisks indicate amino acid identities between S6 segments. (B) Helical wheel depiction of KCNQ1-S6 with the two residues critical for KCNE4 modulation (K326 and T327) marked with arrows; the two residues critical for KCNE1 and KCNE3 modulation (S338 and F340) are marked with filled circles. The helical wheel representation of KCNQ1-S6 was produced using HeliQuest software (http://heliquest.ipmc.cnrs.fr/). (C) Side and top views of the KCNQ1 channel and the KCNE1 TMD (orange ribbon). The S1–S5 segments for each KCNQ1 monomer are shown with gray ribbons, whereas the S6 segments are shown in a different color for each subunit. The K326 and T327 residues are shown as space-filled molecules. The KCNQ1-KCNE1 closed-state model was rendered using CHIMERA software and based upon a previously published model (Kang et al., 2008).

involvement of KCNQ1-S6 in the inhibition by KCNE4 based in part on inferences made from an existing experimentally derived structural model for the closed-state KCNQ1–KCNE1 complex (Kang et al., 2008). In this model, the extracellular end of the KCNE1 TMD docks with KCNQ1 in an intersubunit cleft and resides in close contact with S6 of one subunit and sits on the S5 end of the S4–S5 linker of another subunit (see Fig. 10 C). If the KCNE4 TMD docks in a similar way, interactions of KCNE4 with S6 residues K326 and T327 might effectively "glue" the channel in the closed state by directly or indirectly (i.e., immobilizing the S4–S5 linker) restricting movements of S6 that impair channel activation. Some support for this idea comes from a recent disulfide cross-linking study that indicated that interactions between the extracellular end of S6 and the analogous KCNE1 TMD appear to affect open-state probability (Chung et al., 2009).

Alternatively, KCNE4 inhibition of KCNQ1 may be mediated through direct interactions between the extracellular end of S6 and nearby structures critical for ion permeation (pore helix and selectivity filter). We speculate that the KCNE4 TMD is positioned against S6, such that structures in the outer pore vestibule are distorted and ion conductance is attenuated. This idea is consistent with closed-state homology models of the KCNQ1–KCNE1 complex (Kang et al., 2008) that suggest plausible interactions between the outer S6 segment and the extracellular end of the KCNE1 TMD (Fig. 10 C). A preliminary test of this hypothesis was inconclusive because substitution of intracellular K^+ by Rb^+ or extracellular Na^+ by K^+ or Rb^+ did not yield measurable currents in cells coexpressing KCNQ1 and KCNE4 (not depicted).

KCNE4 acts as tethered TMD

We recently reported that the KCNE4 C terminus is necessary but not sufficient for KCNQ1 inhibition, and that the KCNE4 TMD is required for the full effect (Manderfield et al., 2009). We reconcile the observations that KCNQ1 inhibition by KCNE4 is dependent on both the outer KCNQ1-S6 and the presumed cytoplasmic KCNE4 C terminus by proposing a conceptual model in which KCNE proteins act as variably tethered TMDs. In these models, a specific KCNE C terminus acts cooperatively to position the attached TMD with respect to S6 to produce different functional channel modes. According to this view, the KCNE C terminus anchors the accessory subunit to an intracellular domain of KCNQ1, and this enables the KCNE TMD to be placed in close proximity to KCNQ1-S6. Two recent studies demonstrated interactions between the KCNQ1 and KCNE1 intracellular C termini (Haitin and Attali, 2008; Chen et al., 2009), providing evidence in support of this anchoring hypothesis. Once tethered to the channel, the KCNE TMD either alters gating by interacting with the S6 and the S4–S5 linker, and/or by altering channel conductance by interacting with S6 and nearby structures associated with the selectivity filter. This model is consistent with the requirement by KCNE1 and KCNE4 for their respective C-terminal domains to modulate KCNQ1 and the lack of sufficiency of the KCNE1 and KCNE4 C termini alone for KCNQ1 modulation (Manderfield et al., 2009). In the case of KCNE3, interactions with KCNQ1 may be mediated predominantly by the TMD, as supported by the observation that removal of the KCNE3 C terminus does not greatly perturb the ability of this subunit to modulate KCNQ1 (Gage and Kobertz, 2004).

Our variable tethering model is also consistent with the idea that a specific KCNE TMD may behave differently depending on how it is anchored to the rest of the channel by the KCNE C terminus. This notion is illustrated by KCNE1 and KCNE3 chimeras carrying the KCNE4 C terminus, which act to inhibit rather than activate KCNQ1 (Manderfield et al., 2009), suggesting that the KCNE4 C terminus is able to impose a KCNE4-like interaction between KCNQ1 and the TMD of either KCNE1 or KCNE3.

In summary, our results provide evidence of a dipeptide motif in KCNQ1-S6 that is critical for channel inhibition by KCNE4 and distinct from structures necessary for KCNE1 and KCNE3 modulation of the channel. We conclude that K_V channel functional diversity promoted by KCNE subunits depends in part on structures within the pore-forming domain.

We thank Dr. Nagy for providing the DsRed-MST cDNA and Dr. Shapiro for providing the c-Myc-KCNQ4 cDNA.

This work was funded by National Institutes of Health grants HL077188 (to A.L. George), DC007416 (to C.R. Sanders), and a pre-doctoral fellowship award to L.J. Manderfield from the American Heart Association Southeast Affiliate.

Lawrence G. Palmer served as editor.

Submitted: 27 March 2009
Accepted: 20 July 2009

REFERENCES

Abbott, G.W., and S.A. Goldstein. 2002. Disease-associated mutations in KCNE potassium channel subunits (MiRPs) reveal promiscuous disruption of multiple currents and conservation of mechanism. *FASEB J.* 16:390–400.

Abbott, G.W., S.A.N. Goldstein, and F. Sesti. 2001. Do all voltage-gated potassium channels use MiRPs? *Circ. Res.* 88:981–983.

Barhanin, J., F. Lesage, E. Guillemare, M. Fink, M. Lazdunski, and G. Romey. 1996. $K_{(V)}$LQT1 and lsK (minK) proteins associate to form the $I_{(Ks)}$ cardiac potassium current. *Nature.* 384:78–80.

Bendahhou, S., C. Marionneau, K. Haurogne, M.M. Larroque, R. Derand, V. Szuts, D. Escande, S. Demolombe, and J. Barhanin. 2005. In vitro molecular interactions and distribution of KCNE family with KCNQ1 in the human heart. *Cardiovasc. Res.* 67:529–538.

Chen, J., R. Zheng, Y.F. Melman, and T.V. McDonald. 2009. Functional interactions between KCNE1 C-terminus and the KCNQ1 channel. *PLoS One.* 4:e5143.

Chung, D.Y., P.J. Chan, J.R. Bankston, L. Yang, G. Liu, S.O. Marx, A. Karlin, and R.S. Kass. 2009. Location of KCNE1 relative to KCNQ1

in the $I_{(KS)}$ potassium channel by disulfide cross-linking of substituted cysteines. *Proc. Natl. Acad. Sci. USA*. 106:743–748.

Gage, S.D., and W.R. Kobertz. 2004. KCNE3 truncation mutants reveal a bipartite modulation of KCNQ1 K^+ channels. *J. Gen. Physiol.* 124:759–771.

Gamper, N., J.D. Stockand, and M.S. Shapiro. 2003. Subunit-specific modulation of KCNQ potassium channels by Src tyrosine kinase. *J. Neurosci.* 23:84–95.

Grunnet, M., T. Jespersen, H.B. Rasmussen, T. Ljungstrøm, N.K. Jorgensen, S.P. Olesen, and D.A. Klaerke. 2002. KCNE4 is an inhibitory subunit to the KCNQ1 channel. *J. Physiol.* 542:119–130.

Grunnet, M., S.P. Olesen, D.A. Klaerke, and T. Jespersen. 2005. hKCNE4 inhibits the hKCNQ1 potassium current without affecting the activation kinetics. *Biochem. Biophys. Res. Commun.* 328:1146–1153.

Haitin, Y., and B. Attali. 2008. The C-terminus of Kv7 channels: a multifunctional module. *J. Physiol.* 586:1803–1810.

Hamill, O.P., A. Marty, E. Neher, B. Sakmann, and F.J. Sigworth. 1981. Improved patch-clamp techniques for high-resolution current recording from cells and cell-free membrane patches. *Pflugers Arch.* 391:85–100.

Kang, C., C. Tian, F.D. Sönnichsen, J.A. Smith, J. Meiler, A.L. George Jr., C.G. Vanoye, H.J. Kim, and C.R. Sanders. 2008. Structure of KCNE1 and implications for how it modulates the KCNQ1 potassium channel. *Biochemistry.* 47:7999–8006.

Li, Y., S.Y. Um, and T.V. McDonald. 2006. Voltage-gated potassium channels: regulation by accessory subunits. *Neuroscientist.* 12:199–210.

Lindau, M., and E. Neher. 1988. Patch-clamp techniques for time-resolved capacitance measurements in single cells. *Pflugers Arch.* 411:137–146.

Lundby, A., L.S. Ravn, J.H. Svendsen, S. Hauns, S.P. Olesen, and N. Schmitt. 2008. KCNE3 mutation V17M identified in a patient with lone atrial fibrillation. *Cell. Physiol. Biochem.* 21:47–54.

Lundquist, A.L., L.J. Manderfield, C.G. Vanoye, C.S. Rogers, B.S. Donahue, P.A. Chang, D.C. Drinkwater, K.T. Murray, and A.L. George Jr. 2005. Expression of multiple KCNE genes in human heart may enable variable modulation of $I_{(Ks)}$. *J. Mol. Cell. Cardiol.* 38:277–287.

Ma, K.J., N. Li, S.Y. Teng, Y.H. Zhang, Q. Sun, D.F. Gu, and J.L. Pu. 2007. Modulation of KCNQ1 current by atrial fibrillation-associated KCNE4 (145E/D) gene polymorphism. *Chin. Med. J. (Engl.).* 120:150–154.

Manderfield, L.J., and A.L. George Jr. 2008. KCNE4 can co-associate with the $I_{(Ks)}$ (KCNQ1-KCNE1) channel complex. *FEBS J.* 275:1336–1349.

Manderfield, L.J., M.A. Daniels, C.G. Vanoye, and A.L. George Jr. 2009. KCNE4 domains required for inhibition of KCNQ1. *J. Physiol.* 587:303–314.

McCrossan, Z.A., and G.W. Abbott. 2004. The MinK-related peptides. *Neuropharmacology.* 47:787–821.

Melman, Y.F., A. Domènech, S. de la Luna, and T.V. McDonald. 2001. Structural determinants of KvLQT1 control by the KCNE family of proteins. *J. Biol. Chem.* 276:6439–6444.

Melman, Y.F., A. Krummerman, and T.V. McDonald. 2002. KCNE regulation of KvLQT1 channels: structure-function correlates. *Trends Cardiovasc. Med.* 12:182–187.

Melman, Y.F., S.Y. Um, A. Krumerman, A. Kagan, and T.V. McDonald. 2004. KCNE1 binds to the KCNQ1 pore to regulate potassium channel activity. *Neuron.* 42:927–937.

Panaghie, G., K.K. Tai, and G.W. Abbott. 2006. Interaction of KCNE subunits with the KCNQ1 K^+ channel pore. *J. Physiol.* 570:455–467.

Ravn, L.S., Y. Aizawa, G.D. Pollevick, J. Hofman-Bang, J.M. Cordeiro, U. Dixen, G. Jensen, Y. Wu, E. Burashnikov, S. Haunso, et al. 2008. Gain of function in I_{Ks} secondary to a mutation in KCNE5 associated with atrial fibrillation. *Heart Rhythm.* 5:427–435.

Restier, L., L. Cheng, and M.C. Sanguinetti. 2008. Mechanisms by which atrial fibrillation-associated mutations in the S1 domain of KCNQ1 slow deactivation of I_{Ks} channels. *J. Physiol.* 586:4179–4191.

Sanguinetti, M.C., M.E. Curran, A. Zou, J. Shen, P.S. Spector, D.L. Atkinson, and M.T. Keating. 1996. Coassembly of $K_{(V)}$LQT1 and minK (IsK) proteins to form cardiac $I_{(Ks)}$ potassium channel. *Nature.* 384:80–83.

Schroeder, B.C., S. Waldegger, S. Fehr, M. Bleich, R. Warth, R. Greger, and T.J. Jentsch. 2000. A constitutively open potassium channel formed by KCNQ1 and KCNE3. *Nature.* 403:196–199.

Shamgar, L., Y. Haitin, I. Yisharel, E. Malka, H. Schottelndreier, A. Peretz, Y. Paas, and B. Attali. 2008. KCNE1 constrains the voltage sensor of Kv7.1 K^+ channels. *PLoS. ONE.* 3:e1943.

Smith, J.A., C.G. Vanoye, A.L. George Jr., J. Meiler, and C.R. Sanders. 2007. Structural models for the KCNQ1 voltage-gated potassium channel. *Biochemistry.* 46:14141–14152.

Strutz-Seebohm, N., G. Seebohm, O. Fedorenko, R. Baltaev, J. Engel, M. Knirsch, and F. Lang. 2006. Functional coassembly of KCNQ4 with KCNE-β- subunits in Xenopus oocytes. *Cell. Physiol. Biochem.* 18:57–66.

Tai, K.K., and S.A. Goldstein. 1998. The conduction pore of a cardiac potassium channel. *Nature.* 391:605–608.

Tapper, A.R., and A.L. George Jr. 2001. Location and orientation of minK within the $I_{(Ks)}$ potassium channel complex. *J. Biol. Chem.* 276:38249–38254.

Xu, X., M. Jiang, K.L. Hsu, M. Zhang, and G.N. Tseng. 2008. KCNQ1 and KCNE1 in the I_{Ks} channel complex make state-dependent contacts in their extracellular domains. *J. Gen. Physiol.* 131:589–603.

Yang, Y., M. Xia, Q. Jin, S. Bendahhou, J. Shi, Y. Chen, B. Liang, J. Lin, Y. Liu, B. Liu, et al. 2004. Identification of a KCNE2 gain-of-function mutation in patients with familial atrial fibrillation. *Am. J. Hum. Genet.* 75:899–905.